

# A simple, general algorithm for calculating the irreducible Brillouin zone

Jeremy J. Jorgensen,<sup>1</sup> John E. Christensen,<sup>1</sup> Tyler J. Jarvis,<sup>2</sup> and Gus L. W. Hart<sup>1</sup>

<sup>1</sup>*Department of Physics and Astronomy, Brigham Young University, Provo, Utah, 84602, USA*

<sup>2</sup>*Department of Mathematics, Brigham Young University, Provo, Utah, 84602, USA*

(Dated: April 2, 2022)

Calculations of properties of materials require performing numerical integrals over the Brillouin zone (BZ). Integration points in density functional theory codes are uniformly spread over the BZ despite integration error being concentrated in small regions of the BZ and preserve symmetry to improve computational efficiency. Integration points over the irreducible Brillouin zone (IBZ), the rotationally distinct region of the BZ, do not have to preserve crystal symmetry for greater efficiency. This freedom allows the use of adaptive meshes with higher concentrations of points at locations of large error, resulting in improved algorithmic efficiency. We have created an algorithm for constructing the IBZ of any crystal structure in 2D and 3D. The algorithm uses convex hull and half-space representations for the BZ and IBZ to make many aspects of construction and symmetry reduction of the BZ trivial. The algorithm is simple, general, and available as open-source software.

## I. MOTIVATION

Intrinsic properties of materials, such as the band energy or density of states, require integrals over the Brillouin zone (BZ)<sup>1</sup>. The band energy in density functional theory (DFT) codes<sup>2,3</sup> is normally calculated with a uniform mesh over the BZ using the rectangular integration method. The symmetry of the crystal is used to reduce the number of eigenvalues that must be computed, which is beneficial because the majority of a DFT simulation for a metallic system is spent solving eigenvalues in the self-consistency loop<sup>4</sup>. As the  $k$ -point density increases, the reduction factor for a uniform grid will converge quickly to the number of point operations in the space group<sup>5</sup>. Even with a uniform grid, a non-symmetry-preserving offset may decrease the reduction factor and efficiency of the DFT simulation.

Uniform grids require many more eigenvalues because integration errors are concentrated in small regions of the BZ. Adaptive grids would be computationally more efficient but would break symmetry (very few of the  $k$ -points in the grid would be equivalent to other  $k$ -points in the grid by symmetry). Working within the symmetrically distinct part of the BZ (referred to as the irreducible Brillouin zone or IBZ), one has the freedom to refine regions where integration errors are large while naturally preserving symmetry. Integration within the IBZ allows the use of non-symmetry-preserving grids and non-uniform meshes without reducing the efficiency of calculations of the properties of materials.

In particular, most of the error in the calculation of the band energy is located near the Fermi surface, so placing greater numbers of eigenvalues near the surface significantly improves efficiency when compared to a similarly accurate calculation with a symmetry-preserving uniform grid. Put another way, increasing the number of sample points away from the surface does little to improve band energy accuracy while decreasing simulation efficiency. Because we are no longer concerned with symmetry, there is greater freedom in the shapes of subelements the IBZ can be split into for piecewise polynomial interpolation (for example, it is always possible to split the IBZ, a convex polyhedron, into tetrahedra).

Bands crossings often occur at locations of high symme-

try within the Brillouin zone and introduce fine features in the band structure that are difficult to approximate. Integrating over the irreducible Brillouin zone moves non-accidental crossings to the boundary of the IBZ and effectively removes these discontinuous derivatives, improving the rate of convergence.

There are already algorithms for calculating the BZ<sup>6</sup>, a topic covered in nearly all solid-state physics textbooks. Despite many papers on calculating points and lines of high symmetry in the BZ<sup>7</sup>, we are aware of only one other algorithm<sup>8</sup> for calculating the IBZ that has little explanation and no results for verification. In what follows, we present an algorithm that uses crystal point symmetries to efficiently reduce the Brillouin zone to the irreducible Brillouin zone using only the lattice vectors, the atomic basis, and the crystal symmetries. The algorithm is useful for higher-order integration methods, enabling them to work exclusively within the IBZ. A proof of the algorithm is provided in the appendix, and an implementation of the algorithm is available as open-source software. With a representation of the IBZ, properties of materials may be calculated with greater efficiency because adaptive integration meshes no longer break symmetry.

## II. BACKGROUND

The arrangement of atoms in an infinite crystal can be characterized by its lattice and atomic basis

$$x = An + \mathbf{m}_\alpha \quad (1)$$

where  $x$  is the position of an atom in the crystal,  $A$  is a matrix whose columns are the lattice vectors,  $n$  is a vector of integers, and  $\mathbf{m}_\alpha$  is the offset of the  $\alpha$ th atom in the unit cell. The reciprocal lattice, obtained by taking the Fourier transform of the real-space lattice, satisfies the relation  $AB = I$  (may have a factor of  $2\pi$ , depending on convention) where  $I$  is the identity matrix. A lattice may be thought of as a tessellation of  $\mathbb{R}^3$  where the tile (also known as a “fundamental domain” in mathematics) of the tessellation is called the unit cell. For a single lattice, there are an infinite number of possible tiles that can tessellate  $\mathbb{R}^3$ . The BZ is a unit cell comprising the region of re-

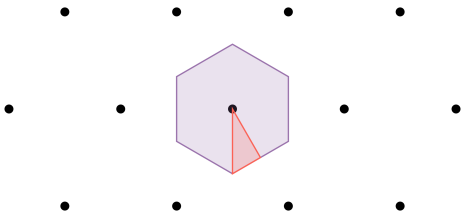


FIG. 1. The Brillouin zone (violet) and irreducible Brillouin zone (red) for a hexagonal lattice. The black dots are reciprocal lattice points.

reciprocal space closer to the origin than to any other reciprocal lattice point.

The BZ takes into account the translational symmetry of the reciprocal lattice. We may take further advantage of symmetry by reducing the BZ with the point symmetries of the crystal (reflections and rotations) to obtain an irreducible Brillouin zone. Just as any point in reciprocal space is equivalent by translation to a point within the BZ, all points within the BZ are equivalent by rotation or reflection to points within the IBZ. A simple 2D illustration of a BZ and IBZ for a hexagonal lattice is shown in Fig. 1.

### III. ALGORITHM

The following is a procedure for generating the Brillouin zone and irreducible Brillouin zone. Although the basic concepts of the Wigner-Seitz construction for the BZ are well known and discussed in most textbooks, they do not provide a practical representation for the BZ or a complete description of the geometry of the BZ (vertices, edges, faces, and volume). A rigorous and general algorithm for calculating the point symmetry reduced Brillouin zone (the irreducible Brillouin zone) and characterizing its geometric features has not been developed to the best of our knowledge. Another novelty of our approach is our use of half-spaces for bisecting lines and planes which eliminate the need to keep track of intersections of planes or lines during the construction process and simplify the logic of the algorithm considerably.

The only inputs required to calculate the IBZ are the lattice vectors, atomic basis, and crystal symmetries. The reciprocal lattice vectors  $B$  are calculated using the relation  $AB = I$  where  $I$  is the identity matrix. The reciprocal lattice vectors are then Minkowski reduced<sup>9</sup> to guarantee that the BZ lies within the set of primitive unit cells that have a vertex at the origin<sup>10</sup> (an example in 2D is shown in Fig. 3). Minkowski reduction reduces the number of reciprocal lattice points that have to be considered during the construction of the BZ, which only becomes a problem when the unit cell is very skew. See Fig. 2 for an example in 2D.

The BZ zone is calculated using the Wigner-Seitz construction (Voronoi tessellation). In 2D, the construction is:

1. Find all the lattice points within a region near the origin.

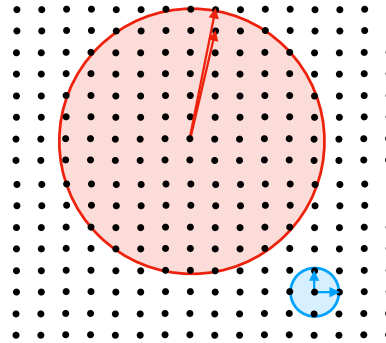


FIG. 2. The utility of Minkowski reduction. The lattice vectors in red and blue both produce the same lattice, shown in black. The calculation of the BZ requires the lattice points within a circle (in 2D) whose radius is the length of the longest lattice vector. When the unit cell is skew, the Minkowski reduced basis results in far fewer lattice points within this circle.

2. For each lattice point, calculate the line that bisects the line drawn from the origin to the lattice point.
3. Determine all points of intersection of bisecting lines and throw away points that lie on the side of any line away from the origin.

(The 3D generalization is straightforward.) Without Minkowski reduction, the number of lattice points needed in the first step is unknown. In many codes, this is han-

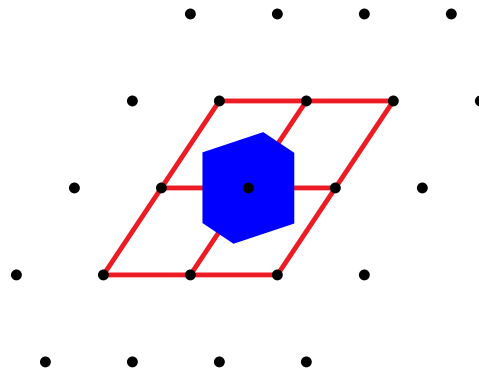


FIG. 3. The Brillouin zone of a 2D lattice lies within the conventional unit cells that have a vertex at the origin when the lattice basis has been Minkowski reduced<sup>a</sup>. Reciprocal lattice points are shown as black points, the unit cells are outlined in red, and the Brillouin zone is shaded in blue.

<sup>a</sup> A basis is Minkowski reduced when the lattice vectors are as short as possible. See 11.

dled by merely considering a large number of lattice points. Minkowski reduction guarantees that the only lattice points needed are those in unit cells that have a vertex at the origin.

Utilizing half-spaces significantly simplifies the calculation of the BZ. With half-spaces, we replace step 3 with calculating the intersection of half-spaces. The lines calculated in step 2 represent the boundary of half-spaces, and the intersection of all the half-spaces gives the BZ. A demonstration of the calculation of the BZ in 2D is shown in Fig. 4.

The point symmetries of the real-space crystal are used to reduce the BZ to the IBZ as follows. We define  $G$  to be the point group of the crystal's space group,  $I \in G$  is the identity operator,  $P$  is the BZ convex polyhedron, and  $V$  is the set of vertices of  $P$ . An outline of the algorithm that reduces the BZ to an IBZ is given below (for  $x, y \in \mathbb{R}^n$  the symbol  $d(x, y)$  denotes the distance between  $x$  and  $y$ ). See the Appendix for more details.

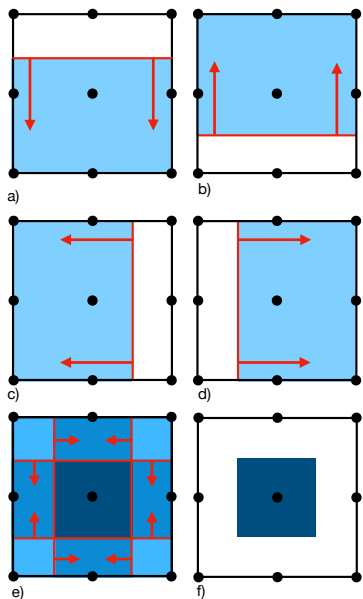


FIG. 4. An illustration of the calculation of the BZ in 2D with half-spaces. In a)-d) are shown the four half-spaces obtained from the four reciprocal lattice points closest to the origin. The boundary of the half-space is outlined in red, and the half-space is shaded in blue. In e) we show the intersection of the four half-spaces. In f) is shown the BZ as a dark blue square.

---

### Algorithm 1 Construct the IBZ from $P$ (the BZ)

---

```

1: procedure CONSTRUCT_IBZ( $M, G$ )
2:    $\triangleright M$  is a set of half-spaces whose intersection is  $P$ .
3:    $\triangleright G$  is the (finite) symmetry group of  $P$ .
4:    $V \leftarrow$  The set of vertices of  $P$ .
5:    $F \leftarrow G \setminus \{I\}$   $\triangleright$  Initialize the set of symmetries.
6:    $N \leftarrow \text{copy}(M)$   $\triangleright$  Initialize the set of half-spaces.
7:   for  $v \in V$  do
8:     for  $g \in F$  do
9:        $v' \leftarrow gv$   $\triangleright$  Calculate the transformed point.
10:      if  $v' \neq v$  then
11:         $H_{v,g} \leftarrow \{x \in \mathbb{R}^n | d(x, v) \leq d(x, gv)\}$ 
12:         $\triangleright$  The half-space bisecting the line segment from  $v$  to  $v'$ 
13:         $N \leftarrow N \cup \{H_{v,g}\}$   $\triangleright$  Insert  $H_{v,g}$  into  $N$ .
14:         $F \leftarrow F \setminus \{g\}$   $\triangleright$  Remove  $g$  from  $F$ .
15:      end if
16:    end for
17:  end for
18:  return  $N$ 
19: end procedure

```

---

We demonstrate reducing the BZ to the IBZ in Fig. 5. When the algorithm finishes, the IBZ is the intersection of the half-spaces in  $N$ , which is returned as a convex hull object. A convex hull object is a convenient way to store vertices, edges, and faces of the IBZ.

We have written the IBZ algorithm in Julia<sup>12</sup> with dependencies on the Julia Polyhedra library<sup>13</sup> and the C qhull package<sup>14</sup>. The code includes functions for visualizing the BZ and IBZ (many of the figures in this paper were produced from it) and can be called from Python.

## IV. TESTING THE IMPLEMENTATION

We know beforehand the relationship between the IBZ volume  $\text{Vol}_{\text{IBZ}}$ , the BZ volume  $\text{Vol}_{\text{BZ}}$ , and the size of the point group  $n_p$ :

$$\text{Vol}_{\text{IBZ}} = \frac{\text{Vol}_{\text{BZ}}}{n_p}, \quad (2)$$

This relation is verified for each IBZ calculation. For testing, we unfold the IBZ. The IBZ is unfolded by applying each operator  $g \in G$  to each of the vertices of the IBZ and then removing duplicate vertices. If the algorithm is working correctly, the unfolded vertices are the same as the vertices of the BZ. Together these two calculations guarantee the IBZ is correct. The second step is necessary because it is possible to get the correct volume reduction but have the wrong shape. The IBZ is not unique, and the IBZ obtained from the algorithm depends on the order of the BZ vertices  $V$  and the order of the point operators  $G$ . In some cases, faces (3D) or edges (2D) of the IBZ may be translationally or rotationally equivalent (see the appendix for a discussion). Plots of the results of the IBZ algorithm for each of the 14 Bravais lattices are shown in Fig. 6 (We only show one BZ and IBZ even though some Bravais lattices have multiple BZ's<sup>15</sup>).

## V. SUMMARY

We have developed an algorithm that can compute an irreducible Brillouin zone (IBZ) of a crystal using the lattice vectors, atomic basis, and crystal symmetries. Working within the IBZ for calculations of properties of materials provides more freedom in selecting points for BZ integrations than uniform grids over the BZ because the grids no longer have to preserve symmetry. In particular, it allows the use of adaptive grids with high sample point densities at locations of high integration error. The calculation of the IBZ is simplified by using convex hull and half-space representations of the IBZ and makes many aspects of the BZ reduction trivial.

## VI. DECLARATIONS

### A. Funding

This work was supported by ONR (MURI N00014-13-1-0635).

### B. Conflicts of interest/Competing interests

The authors have no conflicts of interest that are relevant to the content of this article.

### C. Availability of data and material

Data sharing not applicable to this article as no datasets were generated or analyzed during the current study.

### D. Code availability

The algorithm is a registered Julia package SYMMETRYREDUCEBZ that can also be called from Python.

## VII. APPENDIX

Here we prove that Algorithm 1 is correct for computing an IBZ from the Brillouin zone and the group  $G$  of point operators of the space group of a crystal structure. The algorithm works even when the atomic basis breaks some of the point symmetries of the lattice.

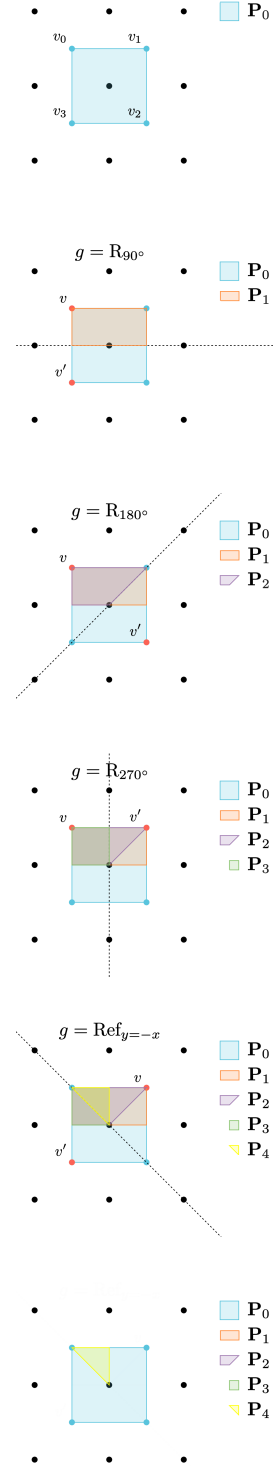


FIG. 5. An illustration of the IBZ calculation. We begin with the BZ labeled  $P_0$ . Each operator in the point group successively reduces the size the BZ. Moving down the figure, we show the reduction of the BZ resulting from selected operators from the point group and end with the IBZ labeled  $P_4$ .

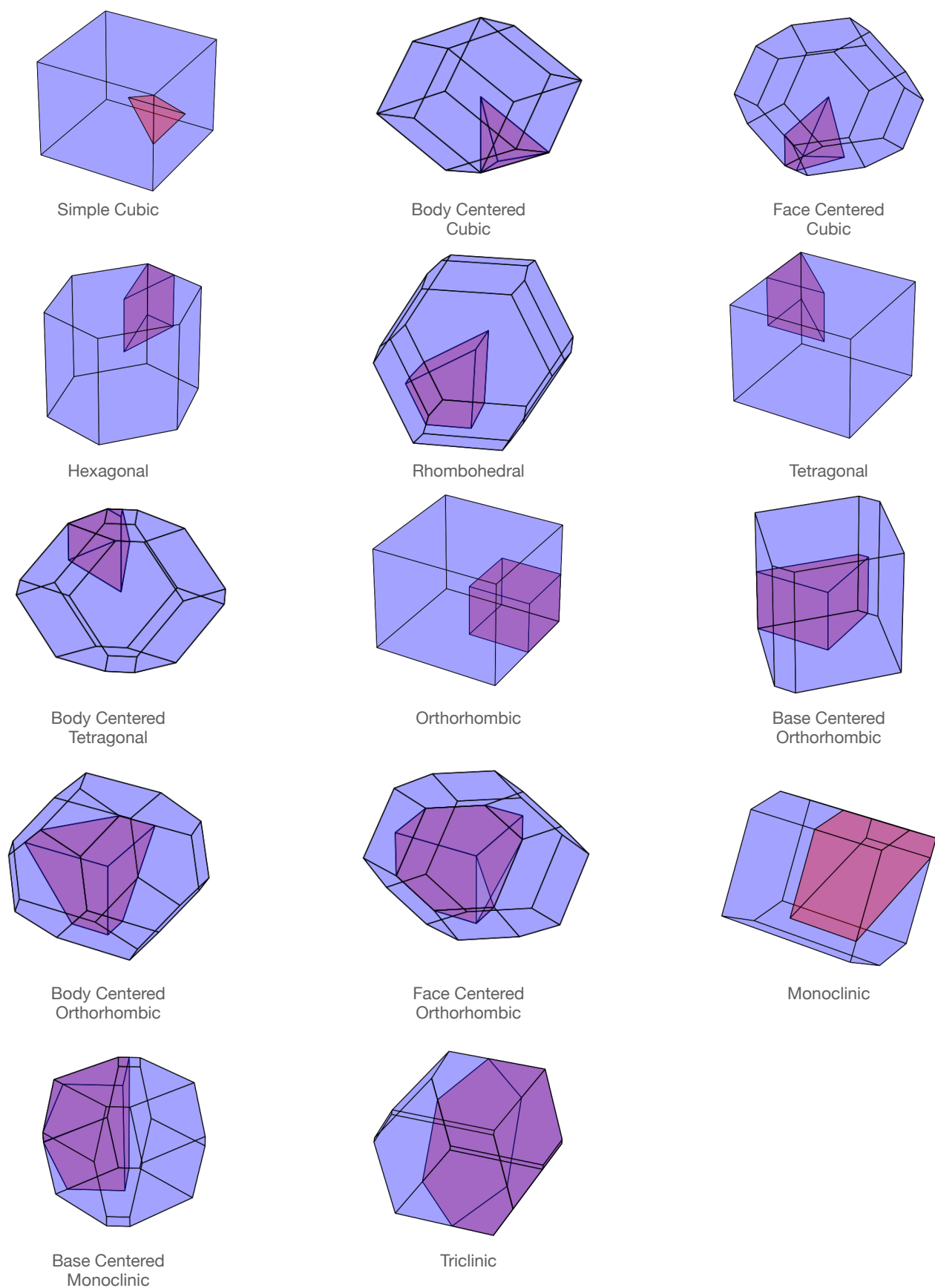


FIG. 6. One BZ and IBZ for each of the 3D Bravais lattices.

To begin we need a precise definition of the IBZ and the interior of a half-space or polytope.

**Definition VII.1.** For any half-space  $H = \{x \in \mathbb{R}^n | d(x, v) \leq d(x, v')\} \subset \mathbb{R}^n$ , the interior  $\mathring{H}$  of  $H$  is the set

$$\mathring{H} = \{x \in \mathbb{R}^n | d(x, v) < d(x, v')\}.$$

For any closed polytope  $Z \subset \mathbb{R}^n$  defined as the intersection  $Z = \bigcap_{H \in \mathcal{C}} H$  of a finite collection  $\mathcal{C}$  of closed half-spaces, the interior  $\mathring{Z}$  of  $Z$  is the set

$$\mathring{Z} = \bigcap_{H \in \mathcal{C}} \mathring{H}.$$

**Definition VII.2.** Given a Brillouin zone (BZ) consisting of a closed polytope  $P \subset \mathbb{R}^n$  with finite symmetry group  $G$ , an irreducible Brillouin zone (IBZ) is a closed polytope  $Q \subset P$  such that

1. For every point  $x \in P$ , there exists a  $g \in G$  such that  $gx \in Q$ .
2. For every point  $y \in \mathring{Q}$  in the interior of  $Q$  and every  $g \in G$ , if  $gy \neq y$ , then  $gy \notin Q$ .

Note that in our definition an IBZ has no interior points that are equivalent under the action of  $G$ , but it can have equivalent faces or edges. Equivalent faces or edges may occur when the crystal structure has fewer point symmetries than the lattice, and they may come up even when the atomic basis does not break symmetry. To find an IBZ without equivalent faces or edges, any face of  $Q$  that is symmetrically equivalent to another face would need to be removed. See Fig. 7 for an example in 2D. For BZ integration, the fact that two faces are equivalent under the action of  $G$  poses no fundamental problem.

**Theorem VII.3.** Assume a finite symmetry group of a polytope  $P$  (the BZ) is  $G \subset O(n)$  (every operator  $g \in G$  acts

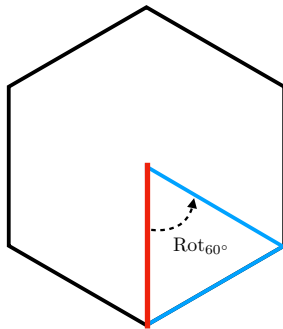


FIG. 7. Example of symmetrically equivalent IBZ edges. In the figure, the BZ is outlined in black and the IBZ in blue. In this example, the atomic basis has broken reflection symmetries; only rotational symmetries remain. The IBZ edge in red is symmetrically equivalent to the opposite edge by a  $60^\circ$  rotation, which is an operation in the point group of a hexagonal lattice.

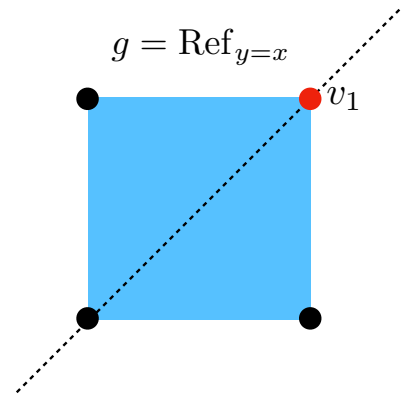


FIG. 8. The stabilizer  $\text{stab}_G(v_1)$  is the set of operators in  $G$  that fix  $v_1$ . Here for the square lattice the reflection  $g = \text{Ref}_{y=x}$  about the line  $y = x$  leaves the point  $v_1$  unmoved ( $v_1 = gv_1$ ), so  $g \in \text{stab}_G(v_1)$ .

linearly and preserves distance in  $\mathbb{R}^n$ ) and that  $P$  is the intersection of a collection  $M$  of half-spaces. Assume further that the group  $G$  acts faithfully on the set  $V$  of vertices of  $P$ , meaning that if  $gv = v$  for all  $v \in V$ , then  $gx = x$  for all  $x \in P$ . Under these assumptions, Algorithm 1 correctly computes an IBZ as the intersection of the half-spaces returned by that algorithm.

*Proof.* Begin by giving  $V = \{v_1, \dots, v_m\}$  the ordering used in the algorithm (in the loop starting at line 7). Let  $G_0 = G$ , and for each  $k \geq 1$  let

$$G_k = \text{stab}_{G_{k-1}}(v_k) = \{g \in G_{k-1} | gv_k = v_k\},$$

be the stabilizer, inside of  $G_{k-1}$  of  $v_k$ ; see figure 8. Let

$$N_k = \{H_{v_k, g}\}_{g \in G_{k-1} \setminus G_k}.$$

Note that  $N_k$  is the set of all the hyperplanes associated to vertex  $v_k$  that are added to  $N$  by the algorithm. Since  $G$  acts faithfully on  $V$ , only the identity element lies in the stabilizer of every vertex, so we have  $F = G \setminus \{I\} = \bigcup_{k=0}^{m-1} G_k \setminus G_{k+1}$ .

If  $N_0 = M$  is the set of hyperplanes defining  $P$ , then the final state of  $N$  is

$$N = \bigcup_{k=0}^m N_k.$$

Let  $P_0 = P$ , and for any  $\ell \geq 1$  let

$$P_\ell = \bigcap_{k=0}^{\ell} \bigcap_{H \in N_k} H$$

be the polytope constructed by intersecting all the hyperplanes added for all the vertices  $v_1, \dots, v_\ell$ . We can characterize the polytope  $P_1$  as

$$\begin{aligned} P_1 &= \{x \in P_0 | d(x, v_1) \leq d(x, gv_1) \forall g \in G_0 \setminus G_1\} \\ &= \{x \in P_0 | d(x, v_1) \leq d(x, gv_1) \forall g \in G_0\}. \end{aligned}$$

And more generally, we can characterize the polytope  $P_\ell$  as

$$\begin{aligned} P_\ell &= \{x \in P_{\ell-1} \mid d(x, v_\ell) \leq d(x, gv_\ell) \forall g \in G_{\ell-1} \setminus G_\ell\} \\ &= \{x \in P_{\ell-1} \mid d(x, v_\ell) \leq d(x, gv_\ell) \forall g \in G_{\ell-1}\}. \end{aligned} \quad (3)$$

The algorithm stops on or before vertex  $v_m$  and returns  $N$ , from which we can construct  $P_m$ , which we show below satisfies the requirements to be an IBZ.

To see that Condition 1 of Definition VII.2 holds, consider any  $x_0 \in P_0 = P$ . For each  $\ell \geq 1$  we will iteratively choose  $g_\ell \in G_{\ell-1} \setminus G_\ell$  such that  $x_\ell = g_\ell x_{\ell-1}$  lies in  $P_\ell$ . Therefore, we will have  $g_m g_{m-1} \cdots g_2 g_1 x_0 \in P_m$ , as required.

For each  $\ell \geq 1$ , assume we are given  $x_{\ell-1} \in P_{\ell-1}$ . Since  $G_{\ell-1}$  is finite, there exists  $g \in G_{\ell-1}$  that minimizes the distance  $d(x_{\ell-1}, gv_\ell)$ ; that is,  $d(x_{\ell-1}, gv_\ell) \leq d(x_{\ell-1}, hv_\ell)$  for any  $h \in G_{\ell-1}$ . Operating by  $g^{-1}$  gives  $d(g^{-1}x_{\ell-1}, v) \leq d(g^{-1}x_{\ell-1}, g^{-1}hv)$  for all  $h \in G_{\ell-1}$ . But the set  $\{g^{-1}h \mid h \in G_{\ell-1}\}$  is equal to the entire group  $G_{\ell-1}$ . Thus we have

$$d(g^{-1}x_{\ell-1}, v_\ell) \leq d(g^{-1}x_{\ell-1}, \gamma v_\ell) \quad \forall \gamma \in G_{\ell-1}. \quad (4)$$

Setting  $g_\ell = g^{-1}$  and using Equations (3) and (4) gives  $g_\ell x_{\ell-1} \in P_\ell$ . Iterating from  $\ell = 1$  to  $\ell = m$  shows that  $g_m g_{m-1} \cdots g_2 g_1 x_0 \in P_m$ , as required. Thus Condition 1 holds.

To see that Condition 2 in Definition VII.2 holds, first note that for every  $v \in V$  if  $g \in F$  satisfies  $gv \neq v$ , then we also have  $g^{-1}v \neq v$ . This implies that if  $H_{v,g} \in N$ , then  $H_{v,g^{-1}} \in N$ . Now consider any  $y \in \mathring{P}_m$  and any operator  $g \in G$  with  $gy \neq y$ . Since  $G$  acts faithfully on  $V$ , there exists at least one vertex  $v \in V$  such that  $gv \neq v$ . Let  $v$  be the first such  $v \in V$  encountered in the loop (at line 7) over vertices in  $V$ , so that  $H_{v,g}$  and  $H_{v,g^{-1}} \in N$ . Since  $y \in \mathring{P}_m$ , we must have  $y \in \mathring{H}_{v,g^{-1}}$ ; hence

$$d(gy, gv) = d(y, v) < d(y, g^{-1}v) = d(gy, v), \quad (5)$$

where the two equalities in (5) follow from the fact that any operator  $g \in G \subset O(n)$  preserves distances in  $\mathbb{R}^n$ . This implies that  $gy \notin H_{v,g}$ , and thus that  $gy \notin P_m$ . Therefore Condition 2 holds.  $\square$

- 
- <sup>1</sup> Éric Cancès, Virginie Ehrlicher, David Gontier, Antoine Levitt, and Damiano Lombardi. Numerical quadrature in the Brillouin zone for periodic Schrödinger operators. *Numerische Mathematik*, pages 1–48, 2020.
- <sup>2</sup> Aron J Cohen, Paula Mori-Sánchez, and Weitao Yang. Challenges for density functional theory. *Chemical reviews*, 112(1):289–320, 2012.
- <sup>3</sup> Tanja van Mourik, Michael Bühl, and Marie-Pierre Gaigeot. Density functional theory across chemistry, physics and biology, 2014.
- <sup>4</sup> Florian Wende, Martijn Marsman, Jeongnim Kim, Fedor Vasilev, Zhengji Zhao, and Thomas Steinke. Openmp in vasp: Threading and simd. *International Journal of Quantum Chemistry*, 119(12):e25851, 2019.
- <sup>5</sup> Wiley S Morgan, John E Christensen, Parker K Hamilton, Jeremy J Jorgensen, Branton J Campbell, Gus LW Hart, and Rodney W Forcade. Generalized regular k-point grid generation on the fly. *Computational Materials Science*, 173:109340, 2020.
- <sup>6</sup> John L Finney. A procedure for the construction of voronoi polyhedra. *Journal of computational physics*, 32(1):137–143, 1979.
- <sup>7</sup> Jason M Munro, Katherine Latimer, Matthew K Horton, Shyam Dwaraknath, and Kristin A Persson. An improved symmetry-based approach to reciprocal space path selection in band structure calculations. *npj Computational Materials*, 6(1):1–6, 2020.
- <sup>8</sup> Alberto Otero-de-la Roza and Víctor Luaña. A fast and accurate algorithm for qtaim integration in solids. *Journal of computational*

*chemistry*, 32(2):291–305, 2011.

- <sup>9</sup> A basis is Minkowski reduced when the lattice vectors are as short as possible. See 11.
- <sup>10</sup> See the appendix of 16.
- <sup>11</sup> Phong Q Nguyen and Damien Stehlé. Low-dimensional lattice basis reduction revisited. *ACM Transactions on Algorithms (TALG)*, 5(4):46, 2009.
- <sup>12</sup> Jeff Bezanson, Alan Edelman, Stefan Karpinski, and Viral B Shah. Julia: A fresh approach to numerical computing. *SIAM Review*, 59(1):65–98, 2017.
- <sup>13</sup> Benoît Legat, Robin Deits, Oliver Evans, Gustavo Goretkin, Twan Koolen, Joey Huchette, Daisuke Oyama, Marcelo Forets, guberger, Robert Schwarz, Elliot Saba, and Chase Coleman. Juliapolyhedra/polyhedra.jl: v0.5.1, May 2019.
- <sup>14</sup> C. Bradford Barber, David P. Dobkin, and Hannu Huhdanpaa. The quickhull algorithm for convex hulls. *ACM Transactions on Mathematical Software*, 22(4):469–483, 1996.
- <sup>15</sup> Wahyu Setyawan and Stefano Curtarolo. High-throughput electronic band structure calculations: Challenges and tools. *Computational materials science*, 49(2):299–312, 2010.
- <sup>16</sup> Gus LW Hart, Jeremy J Jorgensen, Wiley S Morgan, and Rodney W Forcade. A robust algorithm for k-point grid generation and symmetry reduction. *Journal of Physics Communications*, 3(6):065009, 2019.